



## Observations of the Crab Nebula with the Whipple 10 m Telescope

J. GRUBE<sup>1</sup> FOR THE VERITAS COLLABORATION.

<sup>1</sup>*School of Physics and Astronomy, University of Leeds, Leeds, West Yorkshire, LS2 9JT, United Kingdom*

<sup>2</sup>*For full author list see G. Maier, "VERITAS: Status and Latest Results", these proceedings*

*jg@ast.leeds.ac.uk*

**Abstract:** Due to the strong and steady TeV  $\gamma$ -ray emission from the Crab Nebula supernova remnant, its measured flux and energy spectrum can be used to verify the calibration and data reduction methods applied to IACT data acquired over many observing seasons. This gives us confidence in the results obtained on variable TeV sources observed over the same period and in relating the sensitivity of new instruments to historical datasets. Here we present the results of an analysis of 65.3 hours of good quality data taken on the Crab Nebula between October 2000 and March 2006 with the Whipple 10m telescope. The total exposure resulted in a  $46\sigma$  signal with 11886 selected excess events. The energy spectrum was best fit by a power law of the form  $dN/dE = (3.19 \pm 0.07_{\text{stat.}}) \times 10^{-11} \cdot (E/1\text{TeV})^{-2.64 \pm 0.03_{\text{stat.}}} \text{cm}^{-2}\text{s}^{-1}\text{TeV}^{-1}$  in the energy range 0.49–8 TeV. The systematic uncertainty in the flux was estimated to be 30%, with a systematic error of 0.2 in the photon index. A reasonable agreement is shown for a fit to a constant flux over the 6 years.

### Introduction

The Crab Nebula supernova remnant has served as the TeV  $\gamma$ -ray "standard candle" for Imaging Atmospheric Cherenkov Telescopes (IACTs) since its successful detection with a 37 pixel camera on the Whipple 10m telescope in 1989 [1, 2, 3, 4]. Here we provide a record of its flux and energy spectrum from 2000 to 2006 as observed with the Whipple 10m telescope in its current configuration.

The aim of this work is to prove the suitability of various data reduction and analysis techniques and the stability of the instrument for long-term source monitoring. The full study will appear in [5]. Here we compare the results obtained with two sets of Hillas image parameter-based background rejection cuts, "Hard cuts" and "Loose cuts". We discuss errors in energy reconstruction and the variation in effective collection area with the zenith angle of observations, both of which were quantified using simulations. Finally, we plot three integral flux measurements per observing season as a Crab Nebula light curve, and a differential energy spectrum obtained from the combined data set is pre-

sented alongside results from HEGRA, H.E.S.S. and MAGIC.

### Observations

Obs. Period (Month/Year)	$T_L$ (hr)	$N_{\text{Runs}}$	$\langle\Theta\rangle$ (deg.)	$\langle\text{Rate}\rangle$ (Hz)
10/00 - 01/01	13.2	29	18.8	29.7
10/01 - 03/02	23.9	52	17.1	28.0
11/02 - 02/03	8.3	18	17.2	17.6
11/03 - 03/04	5.5	12	17.8	23.5
10/04 - 04/05	5.5	12	15.0	22.0
10/05 - 03/06	8.8	19	18.6	22.8
Total	65.3	142	17.6	25.5

Table 1: Observations of the Crab Nebula.  $T_L$  is the total time ON source,  $\langle\text{Rate}\rangle$  is the mean raw trigger rate.

The Whipple 10 m telescope is operating with a 379 pixel,  $2.6^\circ$  field of view camera. This is the high-resolution inner section of the 490 pixel camera installed in 1999 [6]; the 111 outer guard ring

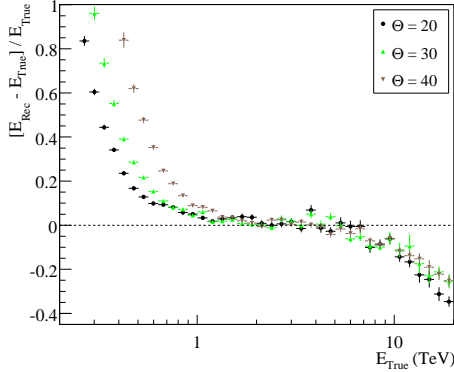


Figure 1: Mean relative error in reconstructed  $\gamma$ -ray energy as a function of simulated energy  $E_{\text{True}}$  at  $20^\circ$ ,  $30^\circ$ , and  $40^\circ$  zenith angle.

pixels were decommissioned in 2003 and consequently have not been included in this analysis.

The Crab Nebula datasets used are listed by season in Table 1. For this systematic study only 28 minute observation runs centered on the source position (ON runs) followed by a matching OFF source run were included. The data cover a range in zenith angle  $\Theta$  of  $10$ – $30^\circ$ . Only data taken under good weather conditions, for which the RMS spread in the raw telescope trigger rate was less than 1.5 Hz were included. As can be seen in Table 1, the average *raw* trigger rate varies somewhat between observing seasons, which is indicative of small changes in telescope efficiency probably due to a combination of instrumental and environmental factors.

## Data Reduction

We applied the Islands method of [7] to extract clean Cherenkov images. The images were parameterized according to image intensity, shape and orientation. The Length and Width were converted to the “reduced scaled” parameters RSL and RSW [2].

A subset of 10 hours of the Crab Nebula observations from 2000–2006 recorded at  $\sim 20^\circ$  zenith angle were used to select two sets of  $\gamma$ -ray selection cuts: Loose cuts and Hard cuts, the latter for measuring a  $\gamma$ -ray flux and energy spectrum with a high detection significance (following equation 17 of [8]). The number of excess  $\gamma$ -ray type events

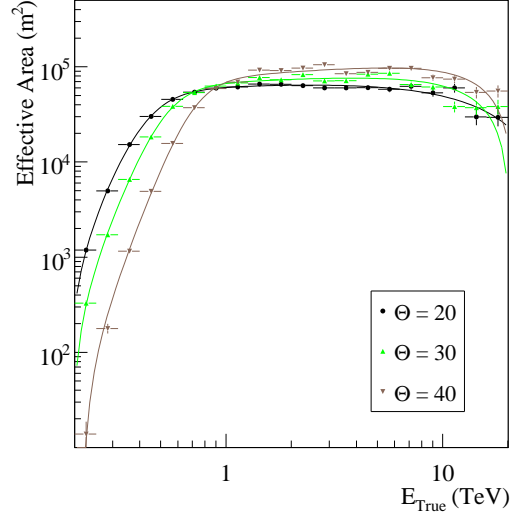


Figure 2: Effective collection area versus true simulated energy after Hard cuts.

$N_\gamma = N_{\text{ON}} - \alpha \cdot N_{\text{OFF}}$  is calculated from number of events passing the cuts, scaled by the ratio of the ON to OFF source exposure time  $\alpha$ . Table 2 lists the multi-parameter selection cuts, corresponding significance and  $\gamma$ -ray detection rate (defined as  $R_\gamma = N_\gamma / T_{\text{ON}}$ ).

## Energy Evaluation and Effective Area

Simulated  $\gamma$ -rays at four zenith angles and three telescope efficiencies  $\mu$  were used to fill lookup tables for the mean simulated energy  $E_{\text{True}}$ , Length, and Width as a function of Distance and  $\text{Log}(\text{Size})$ . A two-dimensional Gaussian smoothing function was applied to the lookup tables with  $\sigma_{\text{Dist}} = 0.05^\circ$  in Distance and  $\sigma_{\text{Log(S)}} = 0.01$  in  $\text{Log}(\text{Size})$ . For each event, the reconstructed energy  $E_{\text{Rec}}$  was calculated from the lookup tables by linearly interpolating between  $\mu$  and  $\cos\Theta$ . Figure 1 shows the mean relative error of the reconstructed energy  $(E_{\text{Rec}} - E_{\text{True}}) / E_{\text{True}}$  as a function of simulated energy  $E_{\text{True}}$  at zenith angles of  $20^\circ$ ,  $30^\circ$ , and  $40^\circ$  after applying Hard selection cuts. At low energies,  $E_{\text{Rec}}$  is overestimated due to events with intensity near the telescope trigger threshold. A usable energy range above  $E_{\text{Safe}}$  with a relative error of  $< 10\%$  was determined for each zenith angle,

Cut	Size (pe)	Distance (deg.)	RSL	RSW	Alpha (deg.)	Len./Size (deg./pe)	$\sigma/\sqrt{\text{hr}}$	$R_\gamma$ ( $\text{min.}^{-1}$ )
Hard	>80	0.2 - 0.95	-2.0 - 1.6	-2.0 - 1.6	<15	<0.0011	5.26	$3.12 \pm 0.18$
Loose	>80	0.2 - 0.95	-2.0 - 2.0	-2.0 - 2.0	<22	–	3.56	$5.51 \pm 0.49$

Table 2: Image selection cuts. The significance  $\sigma/\sqrt{\text{hr}}$  and rate  $R_\gamma$  of selected events are from 10 hours of observations of the Crab Nebula during 2000–2006 at  $\sim 20^\circ$  zenith angle.

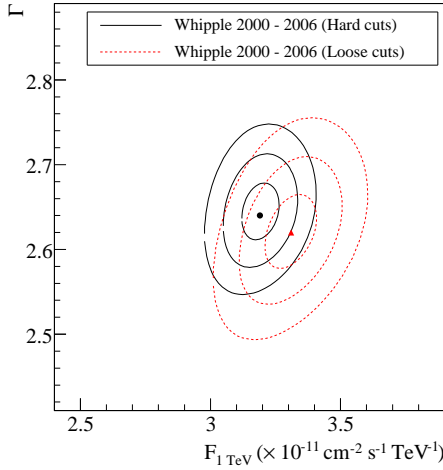


Figure 3: Contour plot of the 68%, 95% and 99.9% confidence intervals from the  $\chi^2$  fit to a power law for the total 2000-2006 dataset after applying Hard cuts or Loose cuts.

with the minimum being  $E_{\text{Safe}} = 0.5$  TeV at zenith angle  $20^\circ$ .

In order to account for biases in energy reconstruction, the energy spectrum is measured using the effective area as a function of reconstructed energy. The maximum distance  $R_o = 400$  m of the simulated air showers from the telescope was chosen to encompass the full impact parameter range of triggered events (0–270 m). The total number of simulated  $\gamma$ -rays is represented by  $N_{\text{sim.}}(E, \Theta, \mu)$ , and the number of detected events passing selection cuts as  $N_{\text{sel.}}(E, \Theta, \mu)$ . The effective areas were fitted with an analytical function modified from equation 3 of [9].

Figure 2 shows the effective areas after Hard cuts as a function of true simulated energy  $E_{\text{True}}$  at zenith angles  $\Theta$  of  $20^\circ$ ,  $30^\circ$ , and  $40^\circ$  with telescope efficiency 85%.

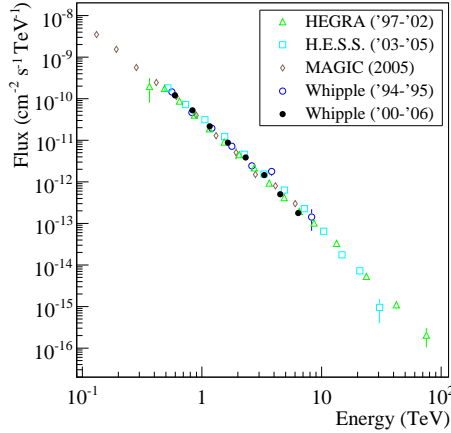


Figure 4: Total 2000–2006 measurement of the Crab Nebula energy spectrum compared to previous measurements.

The integral  $\gamma$ -ray flux above a chosen energy threshold is:

$$F_{>E_{\text{th}}} = - \frac{\left(\frac{dF}{dE}\right)_{\text{th}}}{(1 - \Gamma)} \cdot E_{\text{th}}^{(2-\Gamma)}$$

where a fixed source spectrum with power law photon index  $\Gamma$  is assumed. The excess number of events  $N_\gamma$  is given by:

$$N_\gamma = \frac{dF}{dE} \int_{E_{\text{min}}}^{E_{\text{max}}} \int_0^{T_L} A_{\text{eff}}(E, \Theta(t), \mu(t)) \cdot E^{-\Gamma} dt dE$$

The normalisation factor  $\left(\frac{dF}{dE}\right)_{\text{th}}$  can thus be estimated from the  $N_\gamma$  measured for each run and the integral of the differential rate multiplied by the total livetime of the run  $T_L$ .

## Results and Conclusions

A total Crab Nebula energy spectrum over 2000–2006 was measured with both Hard and Loose selection cuts. Figure 3 shows a contour plot from the  $\chi^2$  fit errors in flux normalization factor  $\left(\frac{dF}{dE}\right)_{\text{th}}$

Dataset (Year)	$\sigma/\sqrt{hr}$	$(\frac{dF}{dE})_{1\text{ TeV}}$	$\Gamma$
'00 - '01	5.32	$3.38 \pm 0.19$	$2.57 \pm 0.10$
'01 - '02	6.19	$3.10 \pm 0.11$	$2.54 \pm 0.06$
'02 - '03	6.91	$2.75 \pm 0.16$	$2.66 \pm 0.11$
'03 - '04	5.21	$3.75 \pm 0.29$	$2.45 \pm 0.10$
'04 - '05	5.54	$2.90 \pm 0.26$	$2.68 \pm 0.19$
'05 - '06	5.28	$3.58 \pm 0.25$	$2.60 \pm 0.12$
Tot. <sub>Hard</sub>	5.64	$3.19 \pm 0.07$	$2.64 \pm 0.03$
Tot. <sub>Loose</sub>	3.48	$3.31 \pm 0.10$	$2.62 \pm 0.04$

Table 3: Energy spectrum of the Crab Nebula with Hard cuts. The power law flux normalization  $(\frac{dF}{dE})$  at 1 TeV is in units of  $10^{-11} \text{ cm}^{-2} \text{ s}^{-1} \text{ TeV}^{-1}$ .

and photon index  $\Gamma$  for the total Whipple 10 m 2000–2006 dataset with Hard and Loose cuts. The best fit values agree at the  $2\sigma$  level. Using Hard cuts, the best fit model was a power law over the energy range 0.49–8 TeV with:

$$\frac{dN}{dE} = (3.19 \pm 0.07) \times 10^{-11} \cdot \left(\frac{E}{1\text{TeV}}\right)^{-2.64 \pm 0.03} \text{ cm}^{-2} \text{ s}^{-1} \text{ TeV}^{-1}$$

Figure 4 shows the corresponding total energy spectrum of the Crab Nebula compared to past measurements with the Whipple 10 m in 1994–1995, HEGRA in 1997–2002, and H.E.S.S. in 2003–2005 [10][2][4].

Table 3 lists the results from a power law fit to the energy spectrum for the individual observing seasons using the Hard cuts (a more comprehensive table including Loose cuts results can be found in [5]). A reasonable agreement in the measured photon index  $\Gamma$  and flux normalization factor  $(\frac{dF}{dE})_{\text{th}}$  is found between data sets within statistical errors. The RMS spread in  $\Gamma$  between datasets is 0.06, with a mean statistical error of 0.11 from each dataset.

The integral flux  $F_{>1\text{TeV}}$  was calculated from the fitted power law spectrum for each dataset. As can be seen in figure 5, the measured values were consistent with steady emission over 6 years; between datasets the RMS spread in the integral flux was 12%. This gives us a sound basis for the characterisation of the flux variability of other sources.

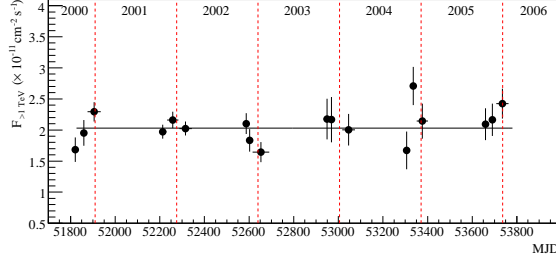


Figure 5: Integral flux of the Crab Nebula over time.

## Acknowledgements

This research is supported by grants from the U.S. Department of Energy, the U.S. National Science Foundation, the Smithsonian Institution, by NSERC in Canada, by PPARC in the UK, and by Science Foundation Ireland.

## References

- [1] F. et al. Aharonian. 5@5 - a 5 GeV energy threshold array of imaging atmospheric Cherenkov telescopes at 5 km altitude. *Astropart. Phys.*, 15:335–356, 2001.
- [2] F. et al. Aharonian. The Crab Nebula and Pulsar between 500 GeV and 80 TeV: Observations with the HEGRA Stereoscopic Air Cerenkov Telescopes. *ApJ*, 614:897–913, 2004.
- [3] F. et al. Aharonian. Observations of the Crab nebula with H.E.S.S. *A&A*, 457:899–915, 2006.
- [4] I. et al. Bond. An island method of image cleaning for near threshold events from atmospheric Cherenkov telescopes. *Astropart.Phys.*, 20:311–321, 2003.
- [5] J. P. et al. Finley. The Granite III upgrade program of the Whipple Observatory. In *Proc.27th ICRC*, volume 7, pages 2827–2830, 2001.
- [6] J. Grube. *PhD Thesis*. University of Leeds, 2007.
- [7] A.M. et al. Hillas. The Spectrum of TeV  $\gamma$  rays from the Crab Nebula. *Astron.J.*, 503:744–759, 1998.
- [8] Y. Li, T. & Ma. Analysis Methods for Results in  $\gamma$ -ray Astronomy. *ApJ*, 272:317–324, 1983.
- [9] R. M. Wagner and et al. Observations of the Crab nebula with the MAGIC telescope. In *Proc.29th ICRC*, volume 4, pages 163–166, 2005.
- [10] T. C. et al. Weekes. Observation of TeV  $\gamma$  rays from the Crab nebula using the atmospheric Cherenkov imaging technique. *ApJ*, 342:379–395, 1989.

This figure "logoblack.png" is available in "png" format from:

<http://arxiv.org/ps/0709.4300v1>